

Article

Characterization of Overburden Deformation and Subsidence Behavior in a Kilometer Deep Longwall Mine

Manoj Khanal ^{1,*}, Qingdong Qu ^{1,*}, Yiran Zhu ^{1,2}, Jianlin Xie ³ , Weibing Zhu ⁴, Tao Hou ⁵ and Shikang Song ⁵¹ CSIRO Minerals, 1 Technology Court, Pullenvale, Brisbane 4069, Australia; yiran.zhu@csiro.au² School of Earth and Environmental Sciences, The University of Queensland, St. Lucia, Brisbane 4072, Australia³ State Key Laboratory of Coal Resources and Safe Mining, China University of Mining and Technology, Xuzhou 221116, China; xjlincumt@163.com⁴ School of Mines, China University of Mining and Technology, Xuzhou 221116, China; zweibing@163.com⁵ Shaanxi Zhengtong Coal Industry Co., Ltd., Xianyang 713600, China; houtao202204@163.com (T.H.); songsk1981@163.com (S.S.)

* Correspondence: manoj.khanal@csiro.au (M.K.); qingdong.qu@csiro.au (Q.Q.)

Abstract: A thorough understanding of mining-induced overburden deformation characteristics and the associated stress redistributions are essential to effectively manage complex safety and environmental issues that arise from underground mining. This is particular for mining in deep environments. This paper presents a numerical modelling study on a kilometer-deep longwall coal mine where a thick sandstone aquifer is situated approximately 200 m above the working seam. The mine adopts a special mine layout with narrow and wide pillars between longwalls and areas to manage water inrush and coal burst risks. The modelling results show that overburden deformation stops at a certain height, above which the displacement profile over multiple longwall panels become nearly flat. Increasing panel width and extraction height lead to a greater extent of the fractured zone and a larger magnitude of surface subsidence. An extraction height of more than 7 m may breach the thick aquifer. Stress concentration on the wide pillar can undergo up to 5 times increase in the in-situ stress, posing high risks of coal burst. Adjusting mining parameters such as panel width and extraction height can facilitate an effective strategy to minimize water inrush and coal burst risks in such a mining condition.

Keywords: deep mining; aquifer breach; strata movement; longwall excavation; subsidence; coal burst



Citation: Khanal, M.; Qu, Q.; Zhu, Y.; Xie, J.; Zhu, W.; Hou, T.; Song, S. Characterization of Overburden Deformation and Subsidence Behavior in a Kilometer Deep Longwall Mine. *Minerals* **2022**, *12*, 543. <https://doi.org/10.3390/min12050543>

Academic Editor: Yosoon Choi

Received: 4 April 2022

Accepted: 24 April 2022

Published: 27 April 2022

Publisher's Note: MDPI stays neutral with regard to jurisdictional claims in published maps and institutional affiliations.



Copyright: © 2022 by the authors. Licensee MDPI, Basel, Switzerland. This article is an open access article distributed under the terms and conditions of the Creative Commons Attribution (CC BY) license (<https://creativecommons.org/licenses/by/4.0/>).

1. Introduction

With the depletion of shallow mineral resources, the mining operations are going deeper. Coal mining depths in many countries such as China, Germany, Poland, and Russia, have reached more than 1000 m deep [1,2]. In some cases, it is up to 1500 m deep [1]. In China, about 53% of the estimated coal reserves are deeper than 1000 m. Hence, operational and research activities in deep coal mining are progressing rapidly [2–4]. However, the experience in deep mining is limited [5], leading to an increase in mining difficulty and risk associated with the high-stress regime.

There is currently no universally accepted definition of deep mining [6]. Some researchers [1] proposed that deep mining should be defined by the mechanical state characterized by geo-stress, mining-induced stress, and rock mechanical properties [3]. However, the mining depth is commonly used to define deep mining [1–8]. The mines operated below 800 m in coal mining [3] and 1000 m in metal mining [1] are normally considered deep mining.

The complicated geo-mechanical conditions in deep mining present a great challenge for safe, efficient, and environmental-friendly mining. Xie et al. [4] highlighted that the presence of high geo-stress, high geo-temperature, high pore pressure, high risk of rock

and gas burst, high risk of spontaneous combustion, and complicated overburden strata pose safety concerns in deep mining. Further, interrelated dynamic interactions between rock, water, and gas caused by mining adds significant complexity to mine safety and production. Therefore, it is important to gain a clear and thorough understanding of site-specific strata deformation characteristics to implement effective measures to minimize geohazards during and after mining operations.

Coal burst is one of the principal hazards in deep mining. Its risk can be attributed to several factors. In general, rockburst is associated with high static and dynamic loadings [9,10]. The stress concentration in the abutment zones of excavations is the main element for static loading, whereas rock fracturing in overlying and underlying strata is the key source of dynamic loading. Increasing the depth of cover on mining activities and the associated complex local geology can significantly increase the coal burst risk. The properties of the coal being mined also impact the coal burst risk. The burst mechanism in different strengths of coal can be substantially different, suggesting that the same rockburst assessment method may not be applicable to all kinds of coal [11].

The risk of coal burst can be mitigated by optimizing mine designs and extraction parameters. It is reported that a suitable pillar design can significantly reduce coal burst risks [12,13]. The longwall retreat speed also seems to impact the risk of coal burst [14]. The root mechanism underlying these mine design measures are overburden deformation characteristics and their control on stress redistributions. Therefore, it is important to clearly understand overburden deformation processes in specific-mining conditions to develop effective controls for managing coal burst risk.

The overburden deformation and subsidence characteristics in deep mining have been reported to be different from shallow mining [15,16]. The depth of cover acts as one of the several key factors in determining the profile and characteristics of the overburdened strata movement in longwall mining [17]. In addition to the depth of cover, several factors, including stratigraphy, panel dimensions, and thickness of overburden strata, control the development of overburden deformation and stress redistribution. Some researchers pointed out that the number and location of “key strata” [18], defined as competent rock layers, influence the nature of the ground movement. The maximum ground subsidence has a negative logarithmic relation with the mining depth [19–23]. The in-situ stress and tectonic features increase with the mining depth and cause high-stress concentration and intensive failure of the surrounding rock masses during longwall excavations. Thus, the likelihood of rockburst incidents and impact on roadway stability is higher in deep mining than in shallow mining [1,6,7,24,25].

In this paper, a mine in China, operated at an approximate depth of 1000 m, is considered to study the effect of deep longwall mining on overburden strata movement, ground subsidence, and stress redistribution around the pillar region. The CSIRO in-house numerical code, COSFLOW [26], is employed for this study. The effect of mining height, the nature of coal, panel width, and the presence of weak and strong strata on ground deformation characteristics are investigated in this paper. The aim of this study is to provide a qualitative characterization instead of quantitative.

2. Mine Condition

The coal mine studied in this paper is in the Northwest of Shaanxi Province, China. The mining depth is approximately 1000 m. The working seam is up to 14 m thick. A fully mechanized longwall top-coal caving technique is adopted in the mine. The extraction thickness is normally around 6 m in the longwall panels of Area 2. The overburden is dominated by sandstones and mudstones. A thick sandstone aquifer (200 m to 400 m) is located approximately 200 m above the working seam. In addition to coal burst risks in this deep mine condition, the abundant groundwater contained in the aquifer also poses a threat to mining safety, if not managed properly.

The mine has completed the extraction of Area 1, where the longwall panels were 112–150 m wide with varying lengths. A few coal burst incidents were reported during the

mining of Area 1. In addition, the water inflow was up to several hundred cubic meters per hour, causing concerns about water inrush risks. Therefore, the mine needs to manage both the coal burst and water inrush risks in subsequent mining areas.

To reduce the risk of coal bursts and to avoid severe breakage of the thick aquifer, a special design of longwall panel layouts, with narrow pillars between the longwall panels are practiced for Area 2 and 3. These narrow pillars and longwall panels are then separated by a wide pillar. Figure 1 shows the panel layouts in the study area. The current Area 3 of the mine plan is separated from Area 2 by a 200 m wide pillar. The longwall widths, ranging between 180 m and 220 m, are separated by 7 m wide rib pillars in a same mining area. The narrow pillars are meant to suffer failure under abutment stress to avoid stress concentration on the pillar and thereby minimize the risk of coal bursts hazards. The wide area pillar is designed to work as a load-bearing pillar to prevent an extensive breach of the thick aquifer and avoid water inrush risks.

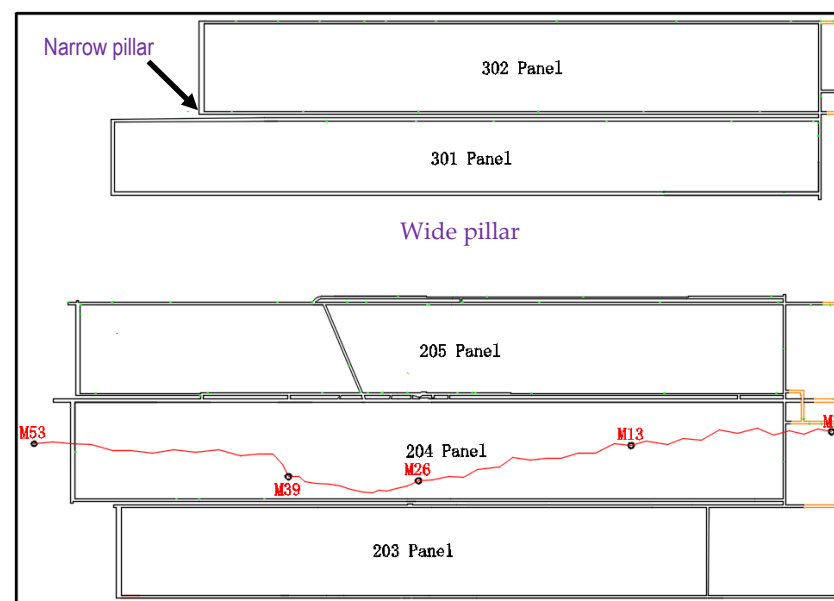


Figure 1. Layout of the longwalls simulated for this study. The layout shows the longwalls separated by narrow pillars in Area 2 (longwall 203–longwall 205) and Area 3 (longwall 301–longwall 302). The two areas are separated by a wide coal pillar. The layout also shows the subsidence survey line along the longwall 204.

3. Model Development and Calibration

An in-house finite element code, COSFLOW [26], is employed in this numerical modelling study. COSFLOW is based on the Cosserat theory, which considers the joint effect on the load deformational behavior of layered rocks. Several studies have demonstrated the efficiency of this approach in simulating strata behaviors in a coal mining environment. More descriptions of COSFLOW and its applications in various mining-related issues can be found in [27,28].

3.1. Model Development

Longwall panels from 203 to 302 are included in the numerical modelling study. Longwall 203 provides a pre-mining condition for longwall 204, which is then used to calibrate the model with respect to the ground subsidence. A 3D view of the numerical model and a pictorial representation of the mine layout is shown in Figure 2. Table 1 lists all the relevant dimensions of the longwall panels. Mining retreats from the southern end of the panels and proceeds towards the north, as shown in the figure with the black arrow. The mining sequence is from longwall 203 to longwall 205, then longwall 302, and finally, longwall 301 (Figure 1).

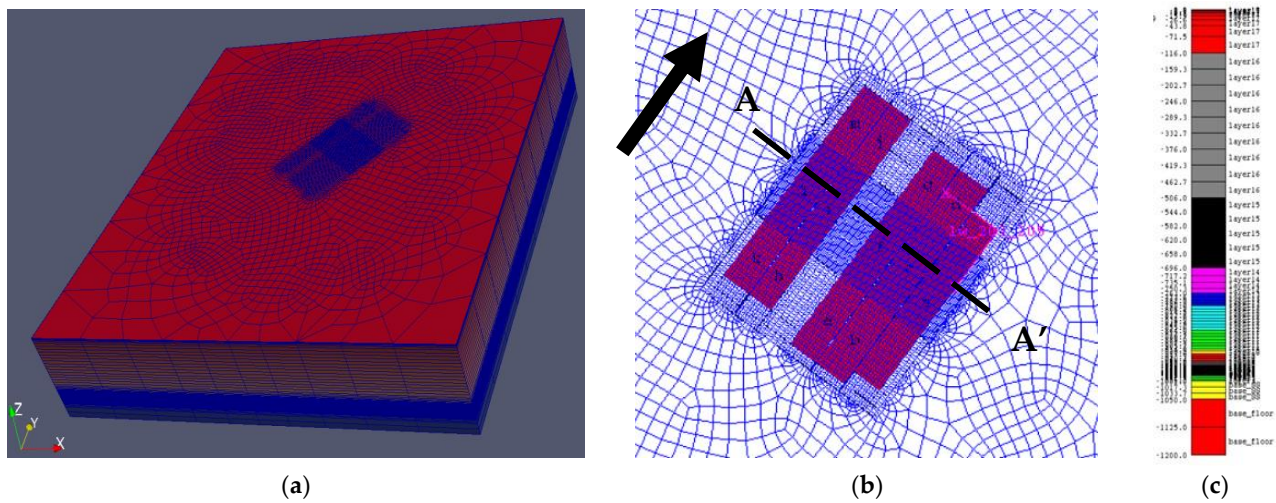


Figure 2. (a) A 3D view of the model and a plan view of the COSFLOW finite-element mesh. The vertical direction has been exaggerated by a factor of 10. (b) The blue lines show the finite-element mesh, which is coarse at the model boundaries and very fine around and above the panels. The cross-section AA' shows the subsidence measurement line on the model. A snapshot of gradually varying mesh along the vertical direction is shown in (c).

Table 1. Quantities defining the panel geometry.

	Length (m)	Width (m)
Longwall 203 pillar	1202.5	180
Longwall 204 pillar	1454.7	7
Longwall 205 “Area Pillar”	1444.5	181
Longwall 301 pillar	1457	220
Longwall 302	1261.4	146
		7
		180

The COSFLOW model is built in a rotated reference frame, as shown in Figure 2, to include the in-situ horizontal stresses aligned with COSFLOW’s “x” and “y” axes. The excavated panels are placed at a minimum of 2 km from the model boundaries to minimize boundary effects. The finite-element mesh is built by sweeping a plan mesh vertically. The number of finite elements in the model is approximately 670,000, consisting of approximately 8500 finite elements on the plan view. Depending on the zone of interest, gradually varying mesh is introduced along the vertical direction. Since the study targets the entire overburden displacement and surface subsidence, finer meshes on the coal seam and immediate roof are not applied to achieve efficient computational time for such a large mine-scale model consisting of five longwall excavations. Nevertheless, a finer-meshed model with more vertical elements was simulated, and the resulting subsidence was very close to the base model.

The geometry used in the numerical model is consistent with the finite-element mesh. The length of the finite elements in the panel width direction is 20 m except for a single mesh to define the 7 m wide pillars. The longitudinal direction mesh is also 20 m except for the zone of 600 m length where the calibration and prediction results are analyzed. The extraction height for longwall 204 in the base model is 6 m. The various stratigraphic layers are collated from the exploration borehole information and interpreted as shown in Table 2. The rock properties used in the model are rescaled from the laboratory-measured data (provided by the mine) based on our experience with the COSFLOW. The Cosserat layered properties are assumed to have joint tension cut-off, joint cohesion, joint dilation angle, and joint friction angle as 0.05 MPa, 0.5 Mpa, 3°, and 25°, respectively.

Table 2. Various strata used in the model and mechanical properties of strata interpreted from the mine measured data for the modelling purpose: SS = Sandstone; MGS = Medium Grain Sandstone; MS = Mudstone; CGC = Coarse Grain Conglomerate; GGS = Fine Grain Sandstone; CGS = Coarse Grain Sandstone.

Layer	Thickness, m	Lithology	Cohesion, MPa	UCS, MPa	Elastic Modulus, GPa	Poisson's Ratio	Tensile Strength, MPa	Rock Dilation Angle, °	Rock Friction Angle, °
17	115.59	Loess/ weathered SS	0.87	3	1	0.25	0.3	5	30
16	390.43	MS, SS	5.05	17.5	8.38	0.25	1.75	5	30
15	189.98	Aquifer, dominated MGS	5.13	18.5	9.36	0.25	5	1.85	32
14	67.02	Aquifer, dominated MGS	5.13	18.5	9.36	0.25	1.85	5	32
13	34.97	Aquifer, dominated MGS	5.05	17.5	8.38	0.25	1.75	5	30
12	66.41	Aquifer, dominated CGS	4.69	18	8.87	0.25	1.8	5	35
11	49.3	Aquifer, dominated CGC and MGS	6.26	21.70	10.28	0.25	2.17	5	30
10	13.3	Aquifer, dominated Sandstone	5.05	17.5	8.38	0.25	1.75	5	30
9	20.08	CGS	6.22	23.9	10.21	0.25	2.39	5	35
8	13.03	Aquifer, dominated MGS	5.13	18.5	9.36	0.25	1.85	5	32
7	10.79	Aquifer, dominated FGS	7.32	28.13	13.98	0.25	2.81	5	35
6	8.95	MS	3.05	11.00	3.73	0.25	1.10	5	32
5	6	COAL	2.33	10	3	0.3	1	4	40
4	1.4	Carbonaceous MS/aluminum MS	5.05	17.5	8.38	0.25	1.75	5	30
3	13.87	MS	5.05	17.5	8.38	0.25	1.75	5	30
2	48.88	Base with FGS	7.32	28.13	13.98	0.25	2.81	5	35
1	150	Elastic							

The density of all the layers is assumed to be 2400 kg/m^3 , except the coal, which has a density of 1300 kg/m^3 . The mechanical properties of each layer in the numerical models are also listed in the table. The constitutive model employed for the rock strata is an elastic, perfectly plastic Mohr-Coulomb Cosserat model, while the constitutive model used for the interlayer interfaces is the Mohr-Coulomb slip model. The working coal seam is set as solid, for which the joint tension cut off and joint cohesion are set very high, and friction angle and dilation angle are set to zero.

The in-situ major horizontal principal stress direction is $25\text{--}35^\circ$ east of north and hence assigned 30° east of north. The longwall excavation direction is in parallel with the major horizontal principal stress direction (shown by a black arrow in Figure 2). The initial vertical stress is assumed to be proportional to the weight of the overburden (an average density of 2400 kg/m^3). The major and minor horizontal stress components are assumed to be 2.36 and 0.84 times the vertical stress, according to the mine measurement data. Roller boundary conditions are prescribed on the model's side and bottom boundaries, while the top is given a stress-free condition.

The numerical model was built using various data collected from the mine and experiences gathered from the previous modelling works using COSFLOW. Features not captured by the rather coarse-scaled stratigraphy are not captured in the numerical model. For instance, pockets of weak strata (should they occur in reality) were not incorporated into the model. In a similar vein, the mechanical properties selected in the calibration model were collated and derived from available reports. The numerical models have not included any explicit faults or joints, apart from the bedding-plane weaknesses described by the Mohr-Coulomb slip model.

3.2. Model Calibration

The ground surface subsidence was the only available data from the mine to calibrate the model. The surface subsidence was surveyed above longwall 204, and the subsidence data for five points along the survey line is shown in Figure 3. These survey points are in and out of the longwall panel. The aim of this calibration is to produce a similar subsidence trend rather than to match the exact data points, as there is only limited data available to compare the magnitudes. The surveyed data show the subsidence of approximately 250–300 mm around and above the mining panels on the ground surface, and there is no significant difference in magnitude between subsidence within and near the longwall goaf. This subsidence profile is different from a typical subsidence profile observed in shallow mining, where substantially large subsidence occurs in the central goaf. Figure 3 also shows that the model predicted ground subsidence. This value and trend are on par with the mine-provided subsidence profile. This confirms that the numerical model behaves similarly to the mining mechanism observed in the field operation.

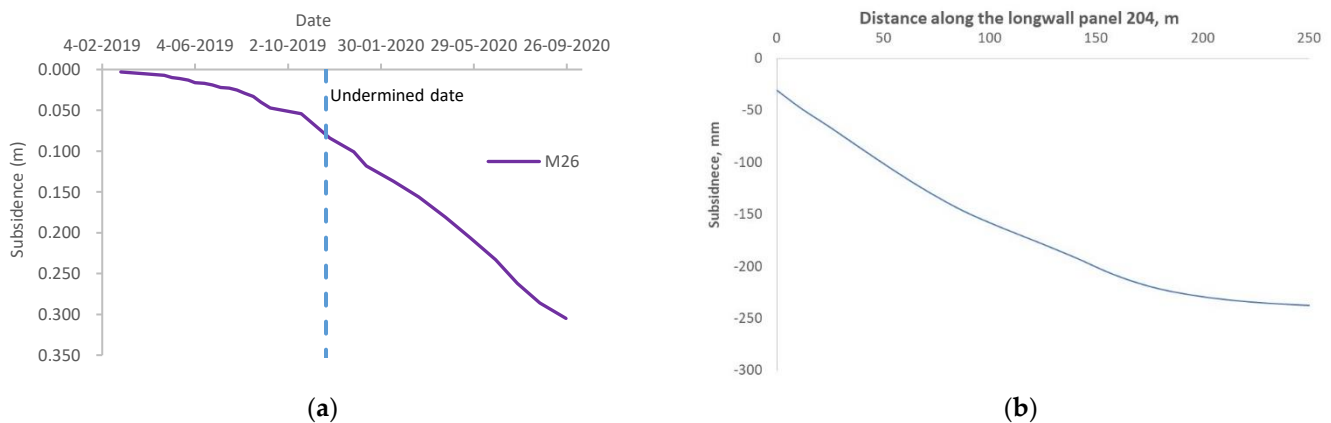


Figure 3. (a) Mine observed subsidence along the panel length during its excavation between May 2019 and September 2020; (b) modelled subsidence along the panel length.

4. Overburden Deformation Characteristics

In the study mine, narrow pillars between longwalls and a wide pillar between Areas 2 and 3 are designed to reduce the risk of coal bursts and minimize the effects of mining on the thick aquifer. Therefore, the deformation characteristics of the overburden strata can have two types of profiles: one is influenced by the narrow pillar between longwalls, and the other is influenced by the wide-area pillar. The characteristics of overburden deformation over these two types of pillars are investigated from the calibrated base model.

4.1. Strata Deformation in Narrow-Pillared Region

The strata deformation from 19 m above the seam roof (960 m below the ground surface) to 180 m above the seam roof (800 m below the ground surface) is shown in Figure 4a. As the distance between the mined seam and strata increases, the magnitude of strata deformation decreases. The displacement profile in the lower section of the overburden shows a trough shape but becomes flat at a certain height above the longwall. For instance, at 19 m above the excavated seam, the roof displacement is around 3.3 m (longwall 203) in the central part of the goaf and reduces towards the edge of the goaf, exhibiting a typical displacement profile. The difference in subsidence between the central goaf and the pillar zone is about 2.8 m. At around 180 m above the excavated seam, the strata displacement profile changes significantly, showing a nearly flat displacement profile (similar to the basin type subsidence profile) across the two panels. This suggests that the strata above this height do not bend and deform significantly. Figure 4b shows the deformation with less than 0.5 m of vertical displacement.

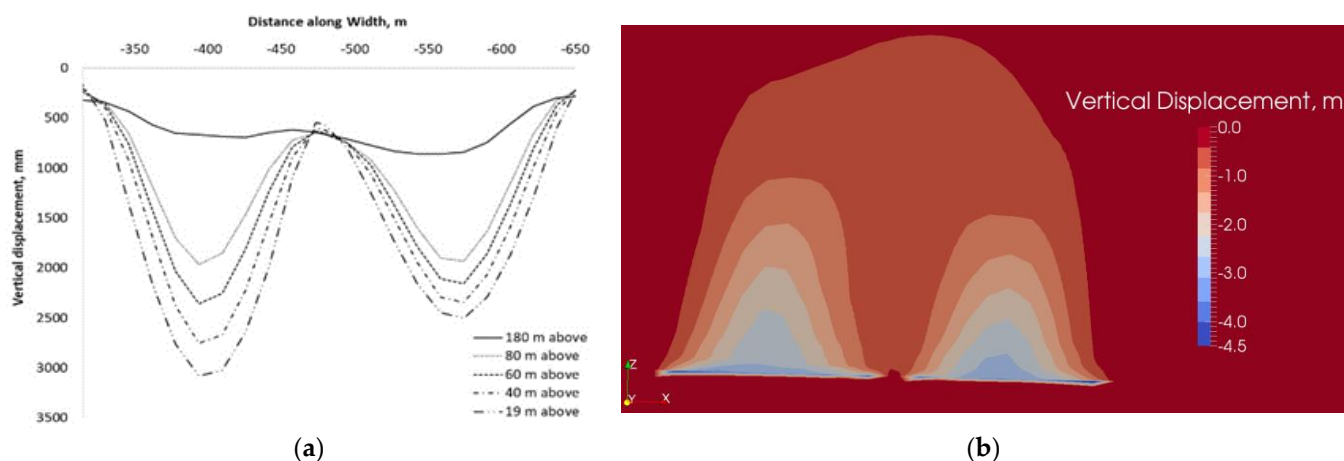


Figure 4. (a) Strata deformation above longwalls 203 (left trough) and 204 (right trough); (b) Sketch of the overburden deformation zone in m.

Based on the interpretation of the characteristics of the overburden strata, the disturbed overburden can be classified in three to four zones [28], for example, the caved zone, the fractured zone, and the continuous deformation zone. These characteristic zones can have different heights depending on the extraction height, mine design, geotechnical, and geomechanical parameters. A tabulated review of the height of disturbance zones in relation to the excavation height is presented in [28].

Accurate delineation of the deformation zones is difficult from the numerical modelling, as the caving and fractures cannot be explicitly identified. In the numerical modelling, the caving of the immediate roof can be reflected by large vertical movements towards the floor of the coal seam elements after they are “deleted” from the model. The height of the fracture zone can be inferred from the magnitude and trend of the vertical strain or displacement. For example, [29] estimated the extent of the deformation zones based on the different magnitude of vertical strains resulting from numerical modelling and showed that the vertical strain greater than 0.98% could be interpreted as the fracture zone.

Figure 5 shows the vertical displacement at different depths along a vertical line in the center of the goaf. The vertical profile clearly shows two deformation zones above and below the depth of -780 m. According to the deformation characteristics, the zone below -780 m (200 m above the worked seam) can be characterized as the fractured zone, where large and continuous vertical strain occurs, and the zone above -780 m as the continuous deformation zone, where vertical strain is minor. The vertical strain of the estimated fracture zone is approximately 1.5%, which agrees with the vertical strain of greater than 0.98% defined in [29].

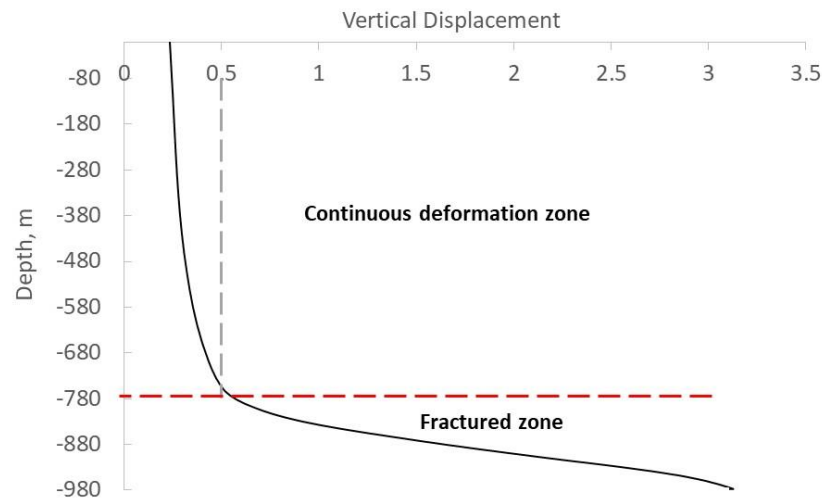


Figure 5. Vertical displacement along the center of the goaf.

In the base case model discussed above, the coal was assumed to be solid (Table 2). For comparison, another model with layered coal is developed. The layered coal [30] is assumed to have a joint tension cut-off, joint cohesion, joint dilation angle, and joint friction angle of 0.05 MPa, 0.5 Mpa, 3° , and 25° , respectively. This comparison provides an effect of the nature of coal on strata deformation characteristics. The two models predict almost identical results in terms of overburden displacement characteristics and the ground surface subsidence (Figure 6). This observation suggests that under the modelled conditions, the nature of coal does not have an impact on the deformation behavior of the overburden strata.

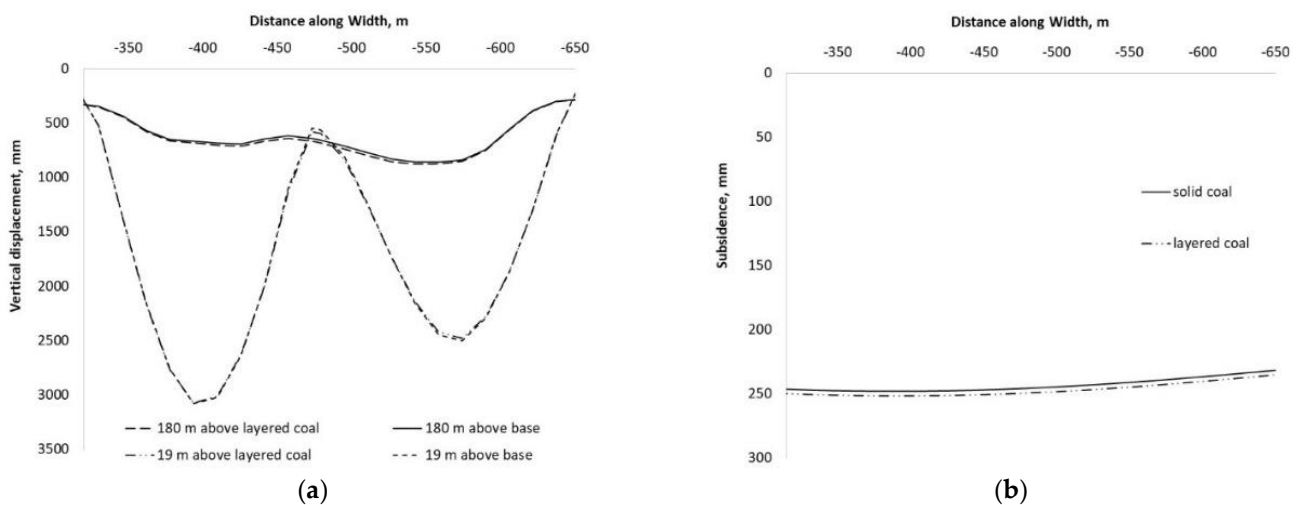


Figure 6. Comparison of strata deformation above longwalls 203 and 204. (a) Vertical displacement at 19 m above the mining seam; (b) ground subsidence.

4.2. Strata Deformation in the Wide Area Pillar Region

After longwall 205, the sequence of longwall excavations is longwall 302 and longwall 301. The results discussed above are based on the simulations after the completion of longwall 205, and the results presented in this section are after the completion of longwall 301 with the solid coal. Figure 7 shows the vertical displacement on different levels across the five longwall excavations. Overburden strata in longwall 203 and longwall 204 continued to deform in the goaf during the subsequent three excavations, causing an increase in the height of the fractured zone (indicated by the level of flat-shaped displacement trough). The additional 540 m wide extraction (333 m from longwall 301, pillar width, and 302; and 181 m from longwall 205) causes the increase in “effective” excavation widths and, as a result, additional deformation of the overburden strata above the panel widths are developed compared to the base model (Figure 4). This causes the fractured zone height to increase. For example, the increment from 180 m to 280 m above the excavation for the fractured zone is witnessed in Figures 4 and 7, respectively.

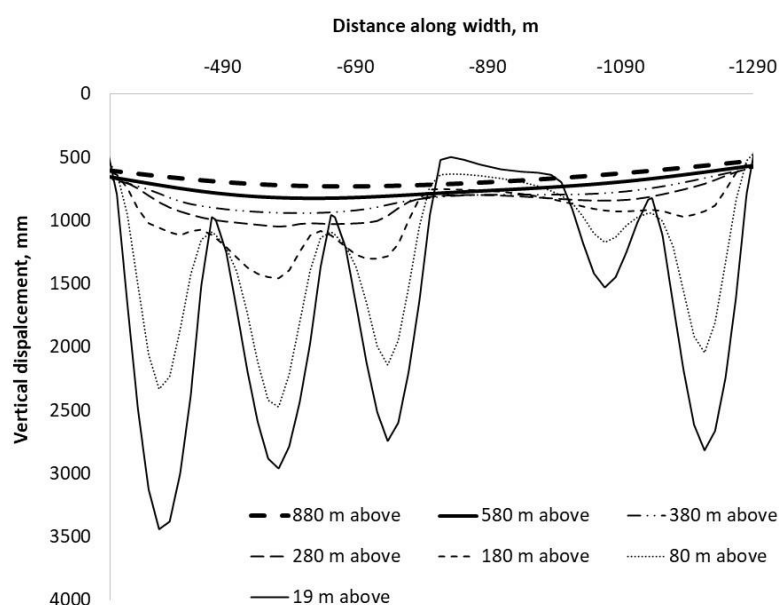


Figure 7. Vertical displacement caused by excavating all five panels (203–302) from left to right. The wide area pillar between longwalls 205 and 301 resist the vertical displacement above this region.

The displacement over the area pillar is smaller than over the narrow pillars, suggesting that the area pillar has not been compressed as much as the narrow pillars and can still take the load, fulfilling the designed purpose. The width of the excavation panels is not uniform. The vertical displacement of the overburden strata above the longwall 301 is smaller than the other panels due to its relatively small width of excavation (146 m). The increment in panel width of 34 m (146 m of longwall 301 to 180 m of longwall 302) causes the increment of 0.2 m vertical displacement at 180 m above the excavation. However, this difference reduces with increasing height and becomes negligible at 280 m above the excavation.

5. Influence of Mining and Geological Factors on Overburden Deformation

The mine has the option to adjust extraction sizes, such as the extraction thickness and panel width, to maximize the production while minimizing the risks of water inrush and coal burst. In addition, the strength of the overburden strata may change significantly in different regions due to geological variations. Moreover, the change in pore pressure within the thick aquifer, whose thickness accounts for more than one-third of the thickness of the entire overburden, could result in the strength variation of the aquifer [31]. These

localized uncertainties in the strata may cause the overburden deformation characteristics to behave incoherently.

5.1. Influence of Panel Width

When the width-to-depth ratio is low (subcritical mining) and all other parameters remain the same, the increase in the excavation width generally causes an increase in the ground surface subsidence [27,28]. Three different excavation widths for longwall 301 are modelled and compared to understand the effect of excavation width on overburden deformation. The excavation widths considered in this study are 147 m (the base case), 200 m, and 268 m. Longwall 301 is mined at the end after longwall 302. Given the model geometry, the increase in width of the longwall 301 panel causes the width of the area pillar to decrease.

In Figure 8, the vertical strata movement caused by the excavation of longwall 301 is the second trough from the right-hand side (highlighted by the rectangular box). As the excavation width increases, the vertical displacement of the roof strata 19 m above the mining seam (represented by the 960 depth curves) increases. For the three cases, the maximum vertical displacement at this level is 1.1 m, 2.5 m, and 3 m, respectively (Figure 8b). As the vertical distance from the strata increases, the difference in the magnitude of vertical displacement lessens among the three cases. For instance, the difference in the vertical displacements at 960 m below the surface (19 m above the longwall) between the base case and the widest panel width is approximately 1.9 m (i.e., 3–1.1 m). The difference reduces to 0.4 m (i.e., 1.2–0.8 m) at 700 m below the ground surface (279 m above the mining seam), and 0.3 m (i.e., 1–0.7 m) at 300 m below the ground surface (679 m above the mining seam).

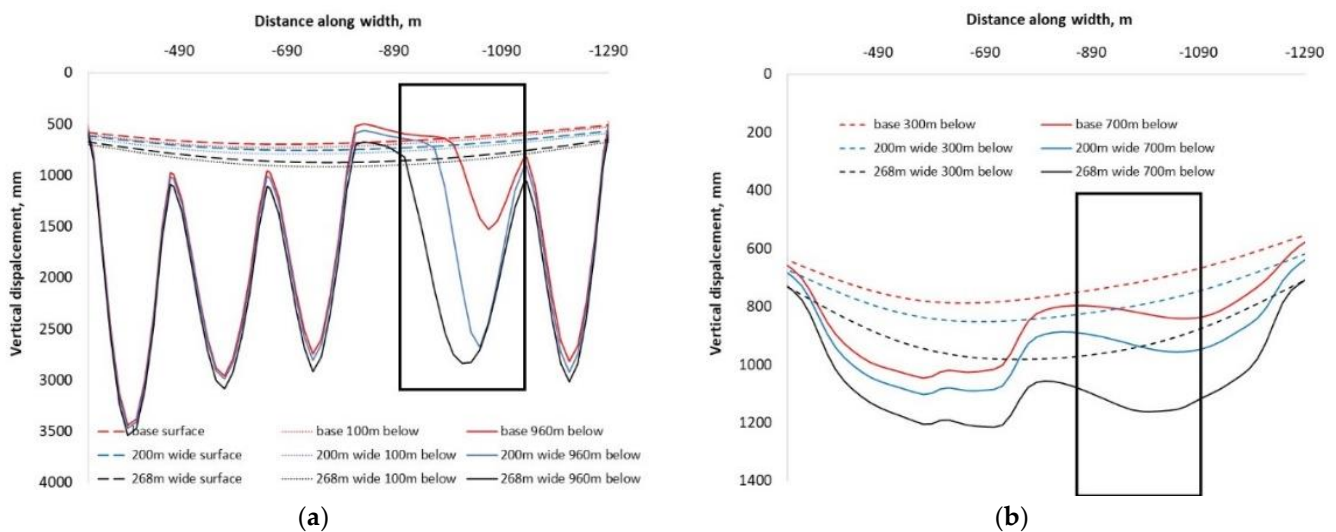


Figure 8. Vertical displacement due to varying excavation widths. (a) at surface, 100 m and 960 m below the ground surface; (b) 300 and 700 m below the ground surface.

As the excavation width increases, the area pillar between longwall 205 and longwall 302 decreases in width in the model. This decrease in pillar width, along with the increase of longwall 302 pillar width, causes the increase in vertical displacement of the strata above the pillar zone (Figure 8a,b). The narrower the pillar width, the larger the subsidence across the mining vicinity. For example, the decrease in pillar width from 220 m to 99 m (due to increasing panel width from 147 m to 268 m) would cause an additional 0.2 m (0.9–0.7 m) subsidence on the ground surface at the lowest point of the subsidence. In this regard, the pillar between Area 2 and Area 3 should have sufficient width to avoid excessive stress concentration in terms of coal burst risk whilst acting as a load-bearing pillar to minimize mining interference with the overburden aquifer. Similarly, Figure 8a compares ground subsidence in all three cases. The wider panel widths with the narrower area panel cause the higher ground subsidence.

5.2. Influence of Extraction Height

The modelled excavation heights are 4 m, 6 m, 7 m, 8 m, 10 m, and 14 m. In the models, the uniform extraction thickness has been assigned. For instance, for the 14 m extraction height model, all five panels have an extraction height of 14 m. The mine may take different extraction thicknesses for individual panels to adjust overburden deformation behavior, for example, excavating 6 m for Area 2 and 10 m for Area 3. The individual extraction height for each panel height in the same model is not studied in this paper.

Figure 9 shows the vertical displacements and ground subsidence caused by increasing excavation height. As excavation height increases, the vertical displacements of the immediate roof and the ground surface increase. The increase in extraction height from 4 m to 14 m causes the maximum ground subsidence to increase from 0.3 m to 2.8 m. In Area 2, the excavation of a series of three panels (equivalent to a total excavation width of 574 m) causes the total subsidence profile to be a typical subsidence trough as that of a longwall panel in the shallow depth (Figure 9b) for more than 8 m of excavation thickness. In Area 3, the ground subsidence over the two narrower panels (333 m width in total) is smaller than that of Area 2. This is evident for extraction heights greater than 8 m of excavation thickness.

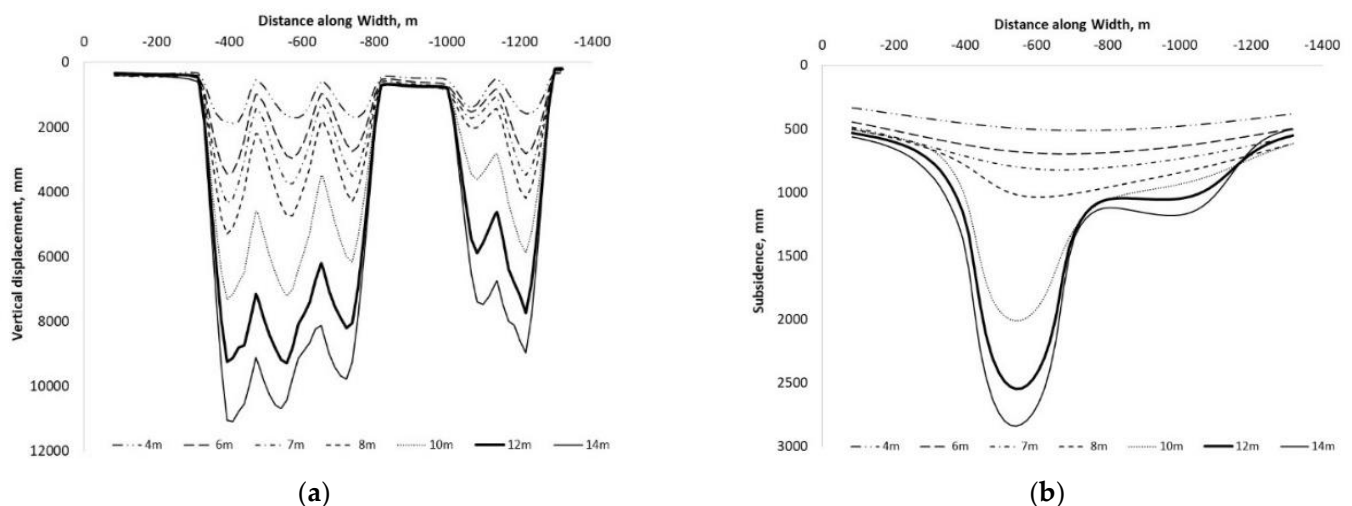


Figure 9. The influence of extraction thickness on overburden movement: (a) 11 m above the mining seam; (b) ground surface.

5.3. Influence of Strata Strength

The effect of strata strength on vertical displacement is investigated by changing the strength properties of the strata listed in Table 2. The cohesion and tensile strength of the strata are halved and doubled from their values in the base model. This is to simulate a potential change of rock strength due to geological variation or change in pore pressure in the thick aquifer caused by water loss. A decrease in pore pressure would result in an increase in strata strength [31] and thus may influence the deformation characteristics.

Figure 10 shows the results of the three cases with different overburden strengths. In these cases, the extraction height is set as 8 m. The stronger strata result in larger ground subsidence over longwall goaves (Figure 10a) and the pillars (Figure 10b) as well. This result could be related to the extent of the fractured zone. The standard empirical formula to estimate the height of fracture zone used in China [32,33] suggests that stronger overburden strata result in a larger vertical extent of the fractured zone. As a result, greater ground subsidence can be induced by the larger fractured zone. The relatively less dilation of strong strata above the fractured zone may also contribute to this phenomenon.

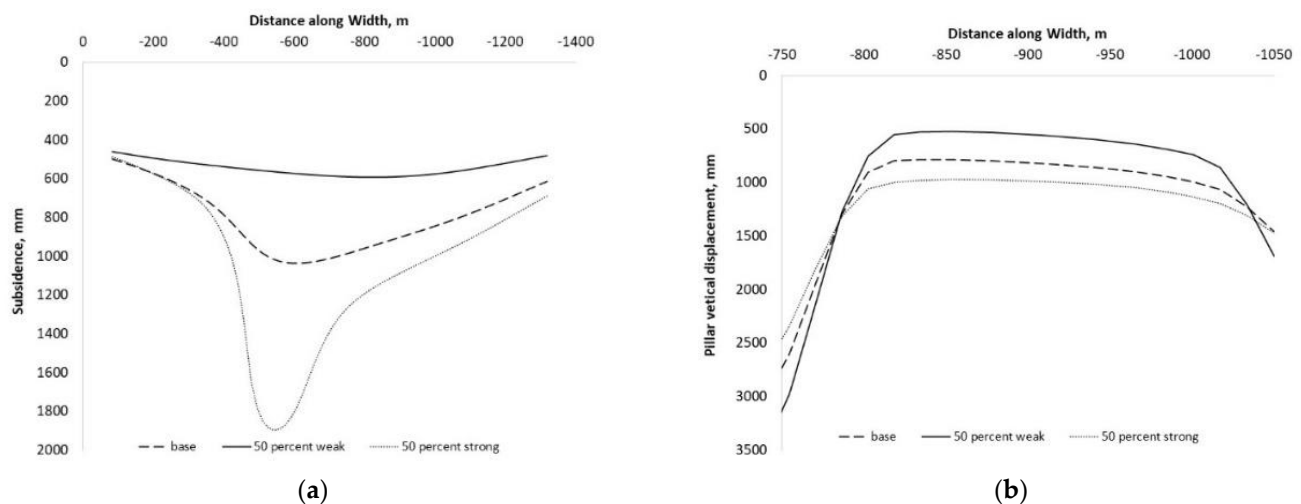


Figure 10. (a) ground subsidence after excavating longwall 302; (b) Vertical displacement at 900 m below the ground surface (77 m above the mining seam) at the pillar.

6. Discussions on Potential Engineering Solutions

The risk of water inrush from the overlying thick aquifers and the risk of coal bursts in the stress concentration region are two major concerns in the study mine. For the former, the risk is related to whether the thick aquifer could break with extensively connected fractures. For the latter, the risk is mostly related to roadways in stress concentration zones. Optimal design and adjustment of longwall dimensions, for example, the extraction thickness and panel width, have the potential to minimize and balance these two risks. A brief discussion on mining interference on the overlying aquifer and the stress concentration on coal bodies is provided in this section.

6.1. Deformation Behaviour of the Aquifer

The potential risk of water inrush has been interpreted from the strata deformation, as the water inrush risk can be associated with the height of the fracture zone. The thick sandstone aquifer of the Luohe Formation is located 200 m above the coal seam in the excavation region. Intensive breakage of the aquifer can result in a large volume of water flowing into the mine workings. The larger extent of the fracture zone cutting through the thick aquifer would result in a higher risk of water inrush at the time of periodic breakage of the overburden. Careful selection of longwall extraction dimensions and a routine assessment of the height of the mining-induced fracture zone are critical. Figure 11 shows the magnitude of the vertical displacement of the stratum located at 270 m above the mining seam, which is approximately 70 m into the aquifer. From the figure, it can be noted that the aquifer may undergo breakage as indicated by the sharp shape and maximum displacement of the displacement trough if the extraction thickness of a series of panels is greater than 7 m. Avoidance of continuous large extraction thickness over a series of longwall panels could help reduce the risk of water inrush.

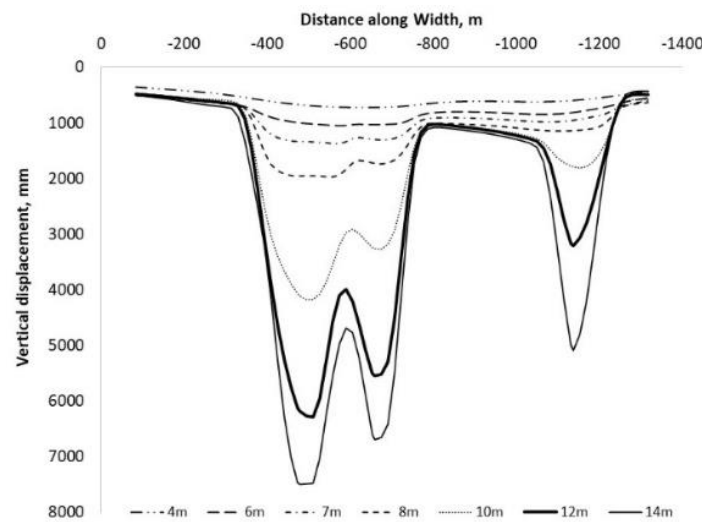


Figure 11. Vertical displacement at 270 m above the mining seam for various extraction heights.

6.2. Stress Concentration

Static loading is a primary factor of the coal burst risk [9,10]. Stress concentration in the abutment zones exhibits the highest static load near underground workings. Stress concentration on the wide Area pillar is analyzed to make a qualitative comparison of the coal burst risk.

Figure 12 shows the stress redistribution over the area pillar after the excavation of longwall 302. The left-hand side of the graph shows the goaf region of longwall 302, while the right-hand side of the graph shows the area pillar between longwall 301 and longwall 205. The peak vertical stress (side abutment stress) in the coal before the mining of longwall 301 is about three times the in-situ stress on both sides of the intact coal. It could further increase to five times the in-situ stress on the longwall 301 goaf side during extraction of the longwall 301. This high-stress concentration results from a combined effect of the side abutment of the neighboring goaf (either longwall 302 or longwall 205) and the front abutment of the active mining (longwall 301). Such increment in the abutment stress can increase the risk of coal burst. It is noted that this model does not include roadways, and therefore the stress environment around the roadways may differ from reality.



Figure 12. Vertical stress development ahead of longwall 301.

Figure 13 shows the vertical stress redistribution across the wide-area pillar under two different extraction thicknesses and overburden strengths. The increase in extraction

thickness appears to have little effect on the magnitude of stress concentration and hence the risk of coal burst. In contrast, high strength of overburden, which may be due to geological variation or reduction of pore pressure, can increase the level of stress concentration and hence increase the risk of coal burst.

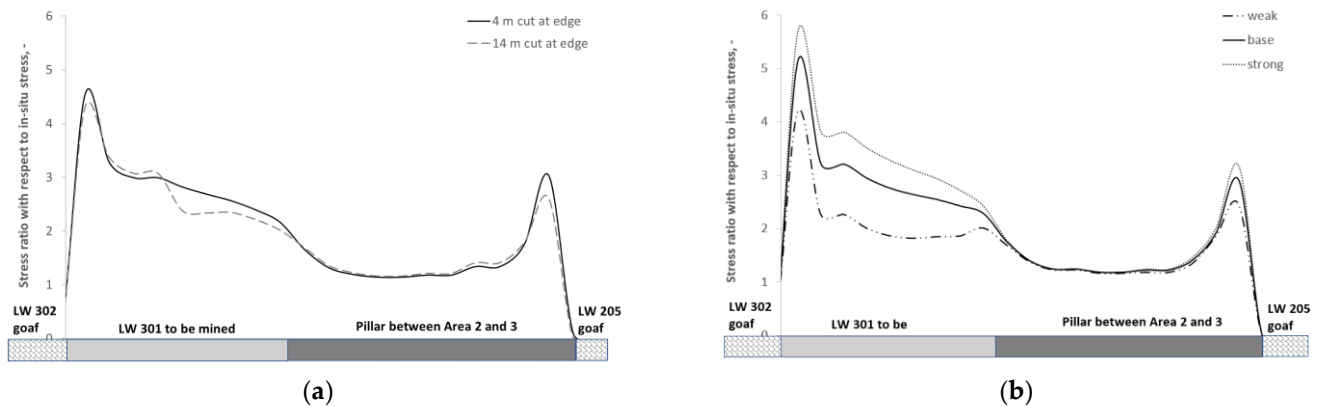


Figure 13. Vertical stress development ahead of longwall 301 under (a) two different cut heights and (b) three different strengths of overburden.

7. Conclusions

The impact of deep longwall operations on strata movement behavior and stress redistribution was investigated with a numerical model. The model was first calibrated with the available subsidence data from the mine, followed by an investigation on the influence of potential changes in mining and geological conditions.

With the extraction thickness less than 8 m, the fractured zone in the overburden is restricted to a certain height, and the overburden further above has minimal deformation resulting in a nearly flat subsidence profile with small magnitude across different panels.

With the extraction thickness greater than 8 m for all the modelled panels, the fractured zone extends to a height that can cause a significant amount of surface subsidence. The cumulative subsidence profile over a series of excavated longwall panels exhibits a trough as that of a single longwall panel. The narrow pillars (7 m wide) between two neighboring longwall panels have little effect on resisting the development of subsidence.

The mine may adjust its extraction parameters, such as panel width and extraction thickness, to balance and minimize the two risks of water inrush from the overlying thick aquifer and coal burst due to stress concentration. Stress concentration over the load-bearing pillar can be up to three to five times the original stress, posing a risk of coal burst. Applying an extraction thickness over 7 m for all panels may breach the thick aquifer located 200 m above the mining seam. Increasing panel width and extraction thickness would result in an increase in the magnitude of the vertical displacement of the overburden strata and, therefore, surface subsidence. Increasing extraction thickness appears to have little effect on the level of stress concentration in the abutment zone. However, the resultant loss of water due to an aquifer breach can increase the stress concentration on coal in abutment zones.

Author Contributions: Conceptualization, Q.Q., J.X., W.Z. and S.S.; methodology, M.K., Q.Q., J.X. and W.Z.; software, M.K. and Q.Q.; validation, M.K., Q.Q. and Y.Z.; formal analysis, M.K., Q.Q. and J.X.; investigation, M.K., Y.Z., T.H., S.S. and Q.Q.; resources, Q.Q., J.X., W.Z., S.S. and T.H.; writing—original draft preparation, M.K., Y.Z.; writing—review and editing, Q.Q., J.X. and W.Z.; funding acquisition, Q.Q. and J.X. All authors have read and agreed to the published version of the manuscript.

Funding: This research is part of a collaborative project between CSIRO and China University of Mining and Technology. The project is funded by Shaanxi Zhengtong Coal Industry Co. Ltd., Shandong Energy, China.

Data Availability Statement: Not applicable.

Acknowledgments: The authors would like to appreciate the help from the colleagues from the China University of Mining and Technology in getting data. The authors would also like to acknowledge Joey Duan for his help in extracting the field data.

Conflicts of Interest: The authors declare no conflict of interest.

References

1. Ranjith, P.G.; Zhao, J.; Ju, M.; De Silva, R.V.S.; Rathnaweera, T.D.; Bandara, A.K.M.S. Opportunities and Challenges in Deep Mining: A Brief Review. *Engineering* **2017**, *3*, 546–551. [[CrossRef](#)]
2. He, M.C.; Xie, H.P.; Peng, S.P.; Jiang, Y.D. Study on rock mechanics in deep mining engineering. *Chin. J. Rock Mech. Eng.* **2005**, *24*, 2803–2813.
3. Xie, H.; Gao, F.; Ju, Y.; Gao, M.; Zhang, R.; Gao, Y.; Liu, J.; Xie, L. Quantitative definition and investigation of deep mining. *J. China Coal Soc.* **2015**, *40*, 1–10.
4. Xie, H. Research framework and anticipated results of deep rock mechanics and mining theory. *Adv. Eng. Sci.* **2017**, *49*, 1–16.
5. Fairhurst, C. Some challenges of deep mining. *Engineering* **2017**, *3*, 527–537. [[CrossRef](#)]
6. Wagner, H. Deep Mining: A Rock Engineering Challenge. *Rock Mech. Rock Eng.* **2019**, *52*, 1417–1446. [[CrossRef](#)]
7. Anderson, T. A comparison of shallow and deep mining. In *Deep Mining 2014: Proceedings of the Seventh International Conference on Deep and High Stress Mining*; Hudyma, M., Potvin, Y., Eds.; Australian Centre for Geomechanics: Perth, Australia, 2014; pp. 181–187.
8. Brown, E.T. Progress and challenges in some areas of deep mining. *Min. Technol.* **2012**, *121*, 177–191. [[CrossRef](#)]
9. Qiu, P.; Ning, J.; Wang, J.; Hu, S.; Li, Z. Mitigating rock burst hazard in deep coal mines insight from dredging concentrated stress: A case study. *Tunn. Undergr. Space Technol.* **2021**, *115*, 104060. [[CrossRef](#)]
10. Dou, L.; Mu, Z.; Li, Z.; Cao, A.; Gong, S. Research progress of monitoring, forecasting, and prevention of rockburst in underground coal mining in China. *Int. J. Coal Sci. Technol.* **2014**, *1*, 278–288. [[CrossRef](#)]
11. Zhang, J.; Jiang, F.; Yang, J.; Bai, W.; Zhang, L. Rockburst mechanism in soft coal seam within deep coal mines. *Int. J. Min. Sci. Technol.* **2017**, *27*, 551–556. [[CrossRef](#)]
12. Mark, C.; Gauna, M. Pillar design and coal burst experience in Utah Book Cliffs longwall operations. *Int. J. Min. Sci. Technol.* **2021**, *31*, 33–41. [[CrossRef](#)]
13. Ahmed, S.S.; Alheib, M.; Gunzburger, Y.; Renaud, V. Pillar Burst Assessment Based on Large-scale Numerical Modeling. *Procedia Eng.* **2017**, *191*, 179–187. [[CrossRef](#)]
14. Zhang, S.; Fan, G.; Jiang, S.; Fan, Z.; Li, S.; Ni, H. Dual-hazard control mechanism of burst-prone and spontaneous combustion coalface considering effect of retreat speed. *Energy Rep.* **2021**, *7*, 278–288. [[CrossRef](#)]
15. Jiang, S.; Fan, G.; Li, Q.; Zhang, S.; Chen, L. Effect of mining parameters on surface deformation and coal pillar stability under cus-tomized shortwall mining of deep extra-thick coal seams. *Energy Rep.* **2021**, *7*, 2138–2154. [[CrossRef](#)]
16. Chen, G.; Wang, Q. Research on Surface Deformation with Increasing Mine Depth. *Adv. Mater. Res.* **2011**, *243*, 5890–5893. [[CrossRef](#)]
17. Xu, J. *Distribution Law of Mining-Induced Strata Fractures and Its Applications*; China University of Mining Technology Press: Xuzhou, China, 2016.
18. Xu, J.; Lian, G.; Zhu, W.; Qian, M. Influence of the key strata in deep mining to mining subsidence. *Mei T'an Hsueh Pao* **2007**, *32*, 686–690.
19. Zhang, J.; Zhang, Q.; Sun, Q.; Gao, R.; Germain, D.; Abro, S. Surface subsidence control theory and application to backfill coal mining technology. *Environ. Earth Sci.* **2015**, *74*, 1439–1448. [[CrossRef](#)]
20. Li, B.; Zhou, N.; Qi, W.; Li, A.; Cui, Z. Surface Subsidence Control during Deep Backfill Coal Mining: A Case Study. *Adv. Civ. Eng.* **2020**, *2020*, 6876453. [[CrossRef](#)]
21. Luan, Y.; Dong, Y.; Ma, Y.; Weng, L. Surface and New Building Deformation Analysis of Deep Well Strip Mining. *Adv. Mater. Sci. Eng.* **2020**, *2020*, 8727956. [[CrossRef](#)]
22. Zhao, G.; Guo, W.; Li, X. Mechanical Properties of Mega-Thick Alluvium and Their Influence on the Surface Subsidence. *Geotech. Geol. Eng.* **2020**, *38*, 137–149. [[CrossRef](#)]
23. Zuoqi, W.; Guoku, W.; Liqin, Z. Study on the Law of Surface Cracks While Coal Mining in the Thin Bedrock and Thick Unconsolidated Layer of Yu-Shen-Fu Mining Area. *E3S Web Conf.* **2018**, *53*, 03040. [[CrossRef](#)]
24. Wu, H.; Wang, X.; Wang, W.; Peng, G.; Zhang, Z. Deformation characteristics and mechanism of deep subsidence coal pillar of the tilted stratum. *Energy Sci. Eng.* **2020**, *8*, 544–561. [[CrossRef](#)]
25. He, M.; Zhang, G.; Wang, G.; Xu, Y.; Wu, C.; Tang, Q. Research on mechanism and application to floor heave control of deep gateway. *Chin. J. Rock Mech. Eng.* **2009**, *28* (Suppl. 1), 2593–2598.
26. Adhikary, D.P.; Dyskin, A.V. A Cosserat continuum model for layered materials. *Comput. Geotech.* **1997**, *20*, 15–45. [[CrossRef](#)]
27. Khanal, M.; Adhikary, D.; Jayasundara, C.; Balusu, R. Numerical Study of Mine Site Specific Multiseam Mining and Its Impact on Surface Subsidence and Chain Pillar Stress. *Geotech. Geol. Eng.* **2016**, *34*, 217–235. [[CrossRef](#)]

28. Khanal, M.; Guo, H.; Adhikary, D. 3D Numerical Study of Underground Coal Mining Induced Strata Deformation and Subsequent Permeability Change. *Geotech. Geol. Eng.* **2019**, *37*, 235–249. [[CrossRef](#)]
29. Guo, H.; Qu, Q.; Adhikary, D. *5-5-Overburden Response to Longwall Mining*; Woodhead Publishing Series in Energy, Advances in Coal Mine Ground Control; Peng, S.S., Ed.; Woodhead Publishing: Sawston, UK, 2017; pp. 111–155.
30. Adhikary, D.P.; Balusu, R.; Khanal, M.; Poulsen, B.P.; Wilkins, A.W.; Farr, I. *Numerical Assessment of Goaf-Hole Instability at Moranbah North Mine*; CSIRO Report EP198160; CSIRO: Canberra, Australia, 2020.
31. Lundborg, N. Strength of rock-like materials. *Int. J. Rock Mech. Min. Sci. Geomech. Abstr.* **1968**, *5*, 427–454. [[CrossRef](#)]
32. *GB51070-2014*; Code for Design of Water Prevention and Control of Coal Mine. China Ministry of Housing and Urban-Rural Development and China General Administration of Quality Supervision, Inspection and Quarantine: Beijing, China, 2014.
33. Xu, Y.; Dai, H. *Subsidence Control and Special Mining*; China University of Mining and Technology Press: Xuzhou, China, 2017.